The corrosion inhibition abilities of PVA and PVP against the corrosion of mild steel in hydrochloric acid

S. Abdulhadi,[1] A. Mohammed,[2] W.K. Al-Azzawi,[3] T. Gaaz,[4]
A.A.H. Kadhum,[5] L.M. Shaker[6] and A.A. Al-Amiery[1,6]*

[1]*Energy and Renewable Technology Centre, University of Technology – Iraq, Baghdad, 10001, Iraq*
[2]*Department of electromechanical engineering, University of Technology – Iraq, Baghdad, 10001, Iraq*
[3]*Al-Farahidi University, Baghdad, 10001, Iraq*
[4]*Department of Machinery Equipment Engineering Techniques, Technical College Al-Musaib, Al-Furat Al Awsat Technical University, Al-Musaib, Babil 51009, Iraq*
[5]*Al-Ameed University, Karbalaa, 56001, Iraq*
[6]*Department of Chemical and Process Engineering, Faculty of Engineering and Build Environment, Universiti Kebangsaan Malaysia, Bangi, Selangor 43600, Malaysia*
**E-mail: dr.ahmed1975@gmail.com*

Abstract

Corrosion inhibitors are chemical compounds that react with the corrosive environment, forming a protective film on the surface of the metal and reducing the rate of corrosion. These inhibitors work by either neutralizing the corrosive environment, inhibiting the corrosion reaction, or both. The introduction of corrosion inhibitors in a corrosive environment aims to reduce the corrosion of well pipes, which are commonly made of mild steel. This method is a reliable and economically beneficial way to combat corrosion. The effects of polyvinyl alcohol (PVA) and polyvinylpyrrolidone (PVP) on the corrosion of mild steel in 1 M hydrochloric acid have been studied using gravimetric techniques and surface morphology analysis. The study investigated the impact of inhibitors concentration, immersion period, and temperature on corrosion rates and inhibition efficiencies for mild steel in HCl conditions. The results showed that PVA has a better inhibition efficiency than PVP at 303 K, with 0.5 mM PVA providing 92.1% protection compared to 0.5 mM PVP which provided 89.4% protection. The inhibition efficiency of PVA increases with increasing concentration but decreases slightly with increasing temperature, while the inhibition efficiency of PVP increases with increasing concentration and temperature. Both inhibitors follow Langmuir adsorption isotherms. Scanning electron microscopy (SEM) was used to examine the surface morphology of the untreated and treated mild steel samples, which showed that both PVA and PVP have the ability to prevent corrosion. A mechanism has been proposed to explain the inhibitory action of PVA and PVP.

Received: November 27, 2022. Published May 29, 2023 doi: 10.17675/2305-6894-2023-12-2-14

Keywords: *PVA, PVP, corrosion inhibitor, corrosion rate, Langmuir isotherm.*

1. Introduction

Due to its exceptional mechanical-chemical properties, mild steel is widely used in various industries, such as construction and engineering. However, its sensitivity to corrosion is a significant problem [1]. To combat this, inhibitors are widely used as additives to prevent mild steel corrosion [2]. The acid pickling process, using mineral acid (HCl), is commonly used in the petrochemical industry to remove mineral oxides and scale depositions [3]. However, this process is still in need of control due to the destructive impact of HCl on corrosion [4]. In order to meet environmental demands, environmentally friendly organic inhibitors have been developed, including inorganic inhibitors such as nitrate, chromate, phosphate, and molybdate, which are widely used for corrosion prevention. Organic compounds also reduce corrosion due to their high electron density centers, which can adsorb on metal surfaces [5–7]. Currently, environmentally safe and sustainable inhibitors are projected to account for 50% of all articles on corrosion inhibitors [8]. Amino acids and their analogues have been shown to have effective corrosion inhibiting characteristics, but they are not widely used due to their cost and ecological impact [9]. Polyvinyl alcohol has a 50–70% inhibitory efficiency as a corrosion inhibitor and was combined with amino acids in previous studies, showing that polymers outperform their monomers as corrosion inhibitors due to more adsorption sites [10–17]. This study assesses the efficacy of polyvinyl alcohol and polyvinyl proline as mild steel corrosion inhibitors in a 1 M HCl environment and examines their performance in relation to concentration, immersion duration, and temperature. Gravimetrical measurements were used to evaluate the enhanced corrosion inhibition of PVA and PVP (Figure 1).

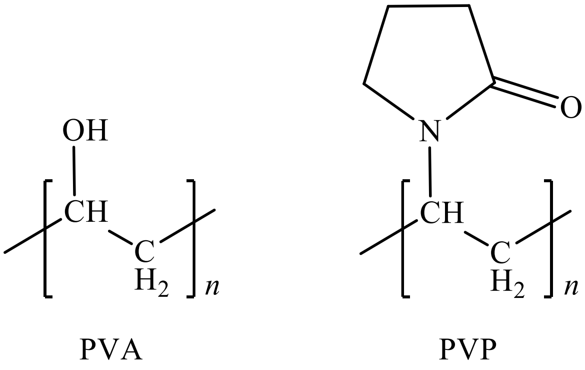

Figure 1. The chemical structures of PVA and PVP.

2. Experimental

2.1. Mild steel samples

Mild steel samples, with dimensions of 4.0 cm×2.5 cm×0.1 cm, were obtained from the company metal samples. Samples with dimensions of 1.0 cm×1.0 cm×0.1 cm were used for gravimetrical techniques. The samples contained the following elements in weight percent: C (0.21), S (0.05), Mn (0.05), Si (0.38), P (0.09), Al (0.01), and Fe (the remainder). The samples were cleaned following the conventional procedure G1-03/ASTM [18], which involved successive cleaning with double distilled water, acetone, and absolute ethanol. The samples were then dried and stored in a desiccator until use.

2.2. Corrosive media

Deionized water was utilized to dilute the analytical hydrochloric acid (37%) obtained from Merck-Malaysia to a concentration of 1 Molar. The corrosive environment consisted of 1 Molar HCl as the corrosive agent. PVA and PVP were added to the corrosive environment as corrosion inhibitors at concentrations of 0.1 mM, 0.2 mM, 0.3 mM, 0.4 mM and 0.5 mM.

2.3. Gravimetric techniques

Gravimetric measurements were performed in 1 M HCl solution with various inhibitor doses for exposure times of 1, 5, 10, 24, and 48 hours at a temperature of 303 K. To assess corrosion, mild steel specimens were immersed in 1 M hydrochloric acid in a 500 ml beaker, kept in a thermostatic water bath. The samples were then removed, cleaned with acetone and deionized water, dried, and weighed. The corrosion rate (C_R) was calculated based on the average weight loss of three test specimens using equation (1) [19]. The effect of temperature was studied by conducting experiments with different concentrations of PVA and PVP for an exposure time of 5 hours.

$$C_{\mathrm{R}}(\mathrm{g\cdot m^{-2}\cdot h^{-1}}) = \frac{\Delta w}{st} \tag{1}$$

The average weight loss of the structural steel, Δw, was calculated in grams. The area of the specimen, s, was expressed in m^2, and the immersion time, t, was measured in hours.

The surface coverage and inhibition efficiency were then determined using equations (2) and (3),

$$\theta = \frac{IE(\%)}{100} \tag{2}$$

$$IE(\%) = \frac{C_{\mathrm{R(0)}} - C_{\mathrm{R(i)}}}{C_{\mathrm{R(0)}}} \tag{3}$$

where $C_{\mathrm{R(0)}}$ is the corrosion rate in untreated environment, $C_{\mathrm{R(i)}}$ is the corrosion rate in treated environment.

2.4. Surface morphology

The surface properties of mild steel specimens in HCl solution were investigated. The scanning electron microscope model, Zeiss MERLIN Compact FESEM, in the electron microscopy unit at UKM was used to study the morphological variations of the surface of mild steel in untreated and treated corrosive media.

3. Results and Discussion

3.1. Gravimetrical analysis

3.1.1. Concentration effects

Figures 2 and 3 present the results of gravimetric measurements for mild steel in untreated and treated 1 M HCl solutions with varying concentrations of PVA and PVP. As HCl is a strong acid, the untreated solution corroded rapidly. However, as the concentration of PVA and PVP increased, the rate of corrosion significantly decreased. The figures demonstrate that PVA and PVP effectively protected the mild steel from the corrosive effects of HCl. The maximum inhibition efficiency was achieved at 0.5 mM, with 92.1% for PVA and 89.4% for PVP.

It is believed that the large molecular structures of PVA and PVP, which contain hetero-elements such as oxygen and nitrogen atoms, help to adhere to the mild steel surface, creating a protective coating. The effectiveness of PVA and PVP as corrosion inhibitors increases with increasing concentrations up to 0.5 mM. However, the inhibition effectiveness remained relatively constant as the concentration approached 1.0 mM. This is due to the adsorption of PVA and PVP particles on the metal substrate. The diversity of functional groups in PVP also plays a role in its ability to prevent corrosion by increasing the electron density of the active sites on the metal surface.

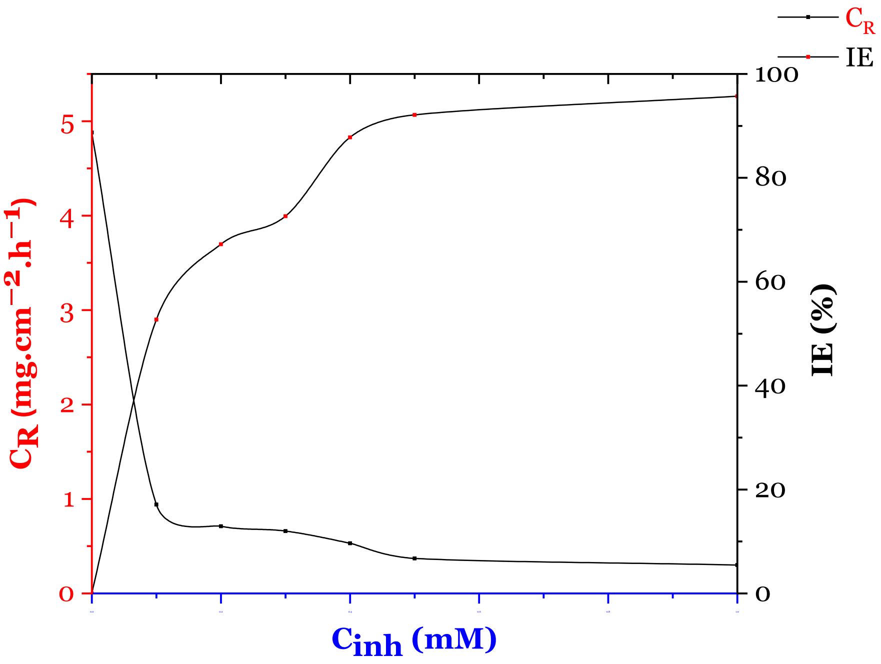

Figure 2. The rate of corrosion and inhibition efficiency for mild steel exposed to 1 M HCl for 5 hours at 303 K was evaluated against various concentrations of PVA.

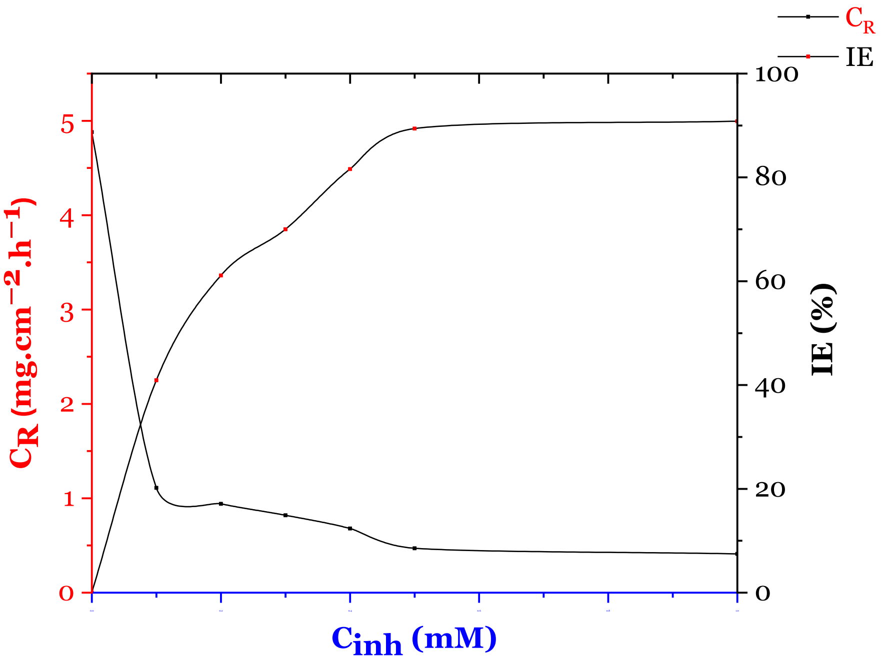

Figure 3. The rate of corrosion and inhibition efficiency for mild steel subjected to 1 M HCl for 5 hours at 303 K was analyzed against various concentrations of PVP.

3.1.2. Immersion time effects

The efficiency of PVA and PVP in reducing corrosion on mild steel was studied by treating 1 M HCl with varying doses of PVA and PVP (0.1 to 1.0 mM) for different exposure times (1 hour to 48 hours) at 303 K. Figures 4 and 5 show the impact of immersion periods on the efficacy of PVA and PVP. During the first 10 hours of immersion, the inhibitory efficacy increases rapidly. Between 10 and 24 hours, it remains fairly stable before gradually declining from 24 to 48 hours. The longer exposure time enhances the inhibitory effectiveness by increasing the amount of PVA and PVP particles adsorbed onto the metallic surface due to higher concentrations. The adsorption density of PVA and PVP particles also significantly increases as a larger number of particles are adsorbed onto the metallic surface, allowing for physisorption (van der Waals forces, hydrogen bonds, or hydrophobic interactions) and chemisorption (coordination interactions between inhibitor molecules and iron atoms on the metallic surfaces). If a few inhibitor molecules leave the surface, the effective area covered by the inhibitor and its inhibitory activity may both decrease. The relatively high inhibitory efficacy observed over a long exposure period demonstrates the stability of the PVA and PVP particles layer adsorbed in an acidic medium.

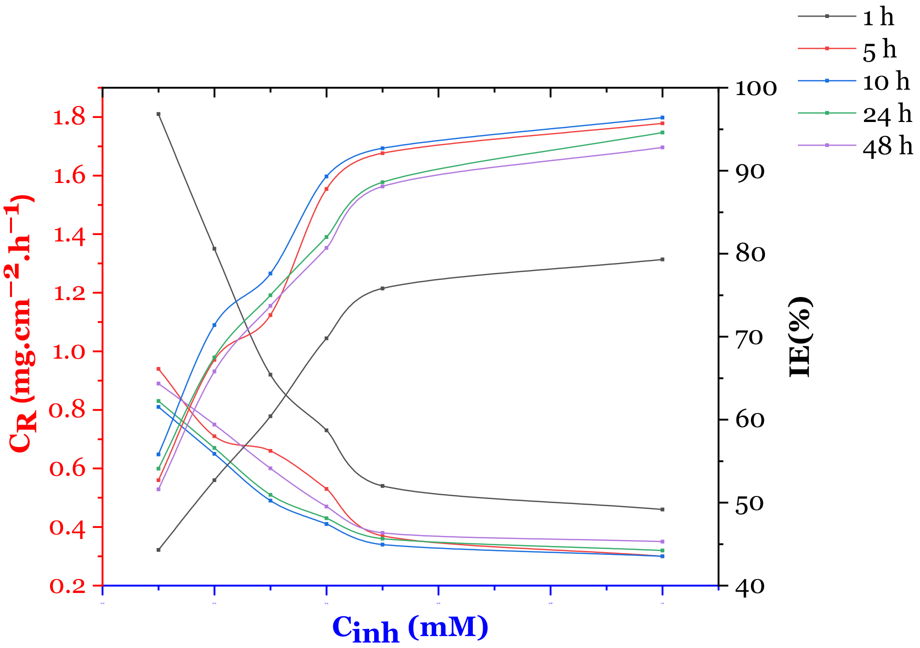

Figure 4. The rates of corrosion and inhibition efficiencies of mild steel exposed to 1 M HCl at 303 K for various immersion times were studied against various concentrations of PVA.

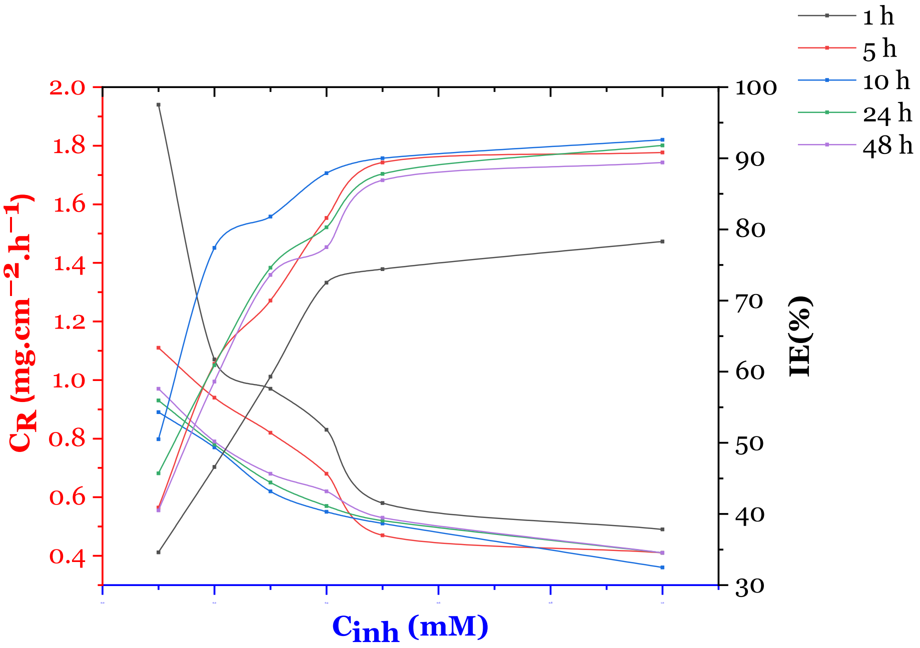

Figure 5. The rates of corrosion and inhibition efficiencies of mild steel exposed to 1 M HCl at 303 K for various immersion times were studied against various concentrations of PVP.

3.1.3. Temperature effects

The inhibition of mild steel corrosion in treated acidic solutions with varying concentrations of PVA (0.1–1.0 mM) and PVP was studied using gravimetric measurements over a 5-hour exposure period and at temperatures ranging from 303 K to 333 K. As the temperature increased from 303 to 333 K, the corrosion rate of PVA increased and its inhibition efficiency decreased, as shown in Figure 6. On the other hand, the corrosion rate of PVP decreased and its inhibition efficiency increased with increasing temperature, as shown in Figure 7. At normal temperature, PVA performed better as a corrosion inhibitor, but PVP showed better inhibitory performance with increasing temperature.

The inhibitory potency of PVA decreased with increasing temperature at all concentrations, suggesting physical adsorption. In contrast, the inhibitory potency of PVP increased with increasing temperature at all concentrations, indicating chemisorption. At high temperatures, PVA particles were also removed from the metal substrate due to adsorption [20]. The inhibition efficiencies of PVA and PVP were studied at 303, 313, 323, and 333 K among other temperatures. At a concentration of 0.5 mM, PVA and PVP showed remarkable inhibition efficiencies of 89.4% and 92.1% at 303 K, respectively. At 303 K, the PVA inhibitor particles at a concentration of 0.5 mM had an efficiency of 92.1%, while at 1.0 mM the efficiency was 95.7%. However, as the temperature increased, the inhibition efficiency decreased.

Figure 6 shows that at the highest concentration (1.0 mM), the PVA inhibitor was less effective when the temperature increased. This result can be explained by physical absorption processes and van der Waals interactions between the PVA particles and the mild steel surface.

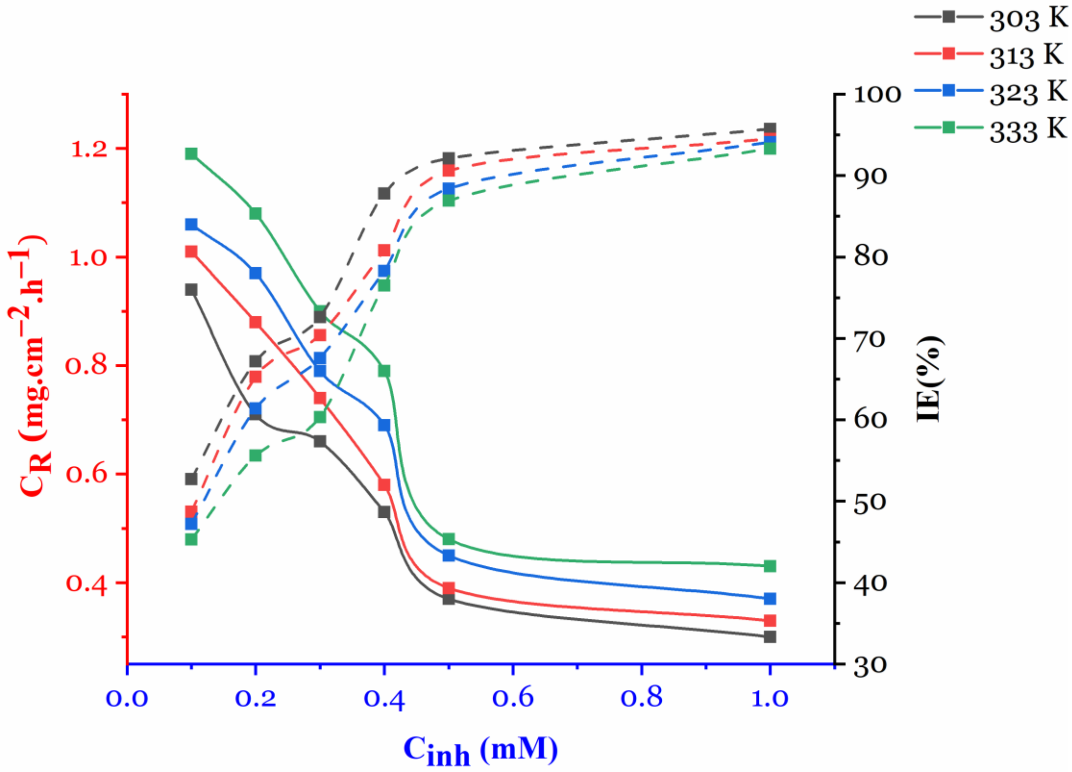

Figure 6. The rate of corrosion and inhibition efficiency for mild steel exposed to 1 M HCl at temperatures ranging from 303–333K for an immersion time of 5 hours were analyzed against various concentrations of PVA.

In addition, at an inhibition concentration of 0.5 mM PVP, the inhibition efficiency was 90.8% at 303 K, 91% at 313 K, 92.8% at 323 K, and 93.7% at 333 K. However, when the inhibitor concentration of PVP was increased to 1 M, the inhibition efficiency decreased slightly to 89.4% at 303 K, 89.8% at 313 K, 91.4% at 323 K, and 92.1% at 333 K, as shown in Figure 7. The figure shows that, even though the inhibition efficacy of PVP increases slightly with increasing temperature (1 mM), it remains at optimum levels. These results can be explained by the chemisorption process, where PVP particles form coordination bonds with the d orbitals of the iron atoms on the surface of mild steel by transferring electron pairs from the heteroatoms of PVP particles to the Fe-orbitals [21].

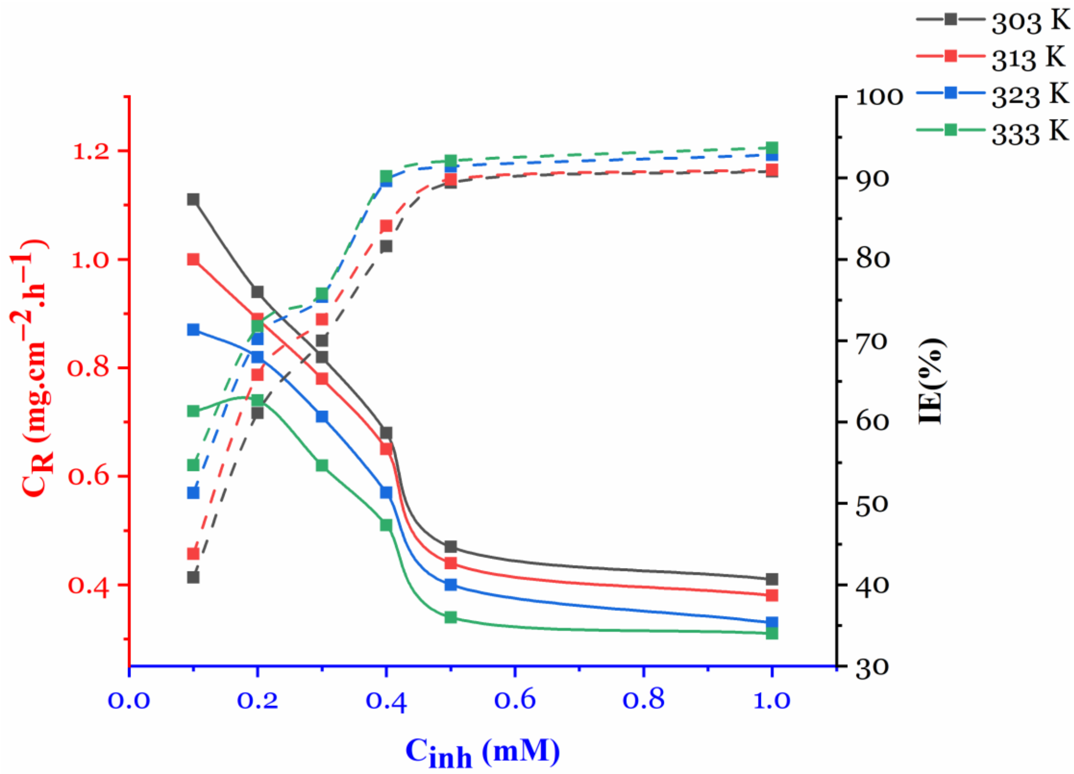

Figure 7. The corrosion rate and inhibition efficiency of mild steel exposed to 1 M HCl at temperatures ranging from 303–333K for a duration of 5 hours were studied against various concentrations of PVP.

In the oil and gas production process, the temperature at the bottom of the well is high, and therefore, a suitable corrosion inhibitor should maintain its effectiveness in corrosive media at high temperatures. Figure 7 for PVP clearly shows that as the temperature increases, the corrosion rate slows, and the effectiveness of the inhibiting agent improves. This is due to the chemical adsorption mechanism where, as the temperature rises, molecules can absorb more energy, causing an increase in average kinetic energy, which in turn allows more PVP particles to adsorb onto the metallic surface [22]. The steady increase in inhibitor concentration also resulted in reduced corrosion rates at the same temperature, indicating that the concentration of both inhibitors is crucial in enhancing surface coverage of inhibitor chemicals, allowing iron atoms to coordinate properly and effectively separate the metallic surface from the HCl environment [23]. Figure 8 compares the inhibitory efficiencies of PVA and PVP in the current study with previously published inhibitors. As far as we know, these inhibitors are friendly to HCl solutions. In the presence of 0.5 mM of PVA and PVP, the inhibition efficiencies reached 92.1% and 89.4%, respectively, at 303 K in a 1 M HCl environment. These results surpass those of some previous inhibitors [24–53].

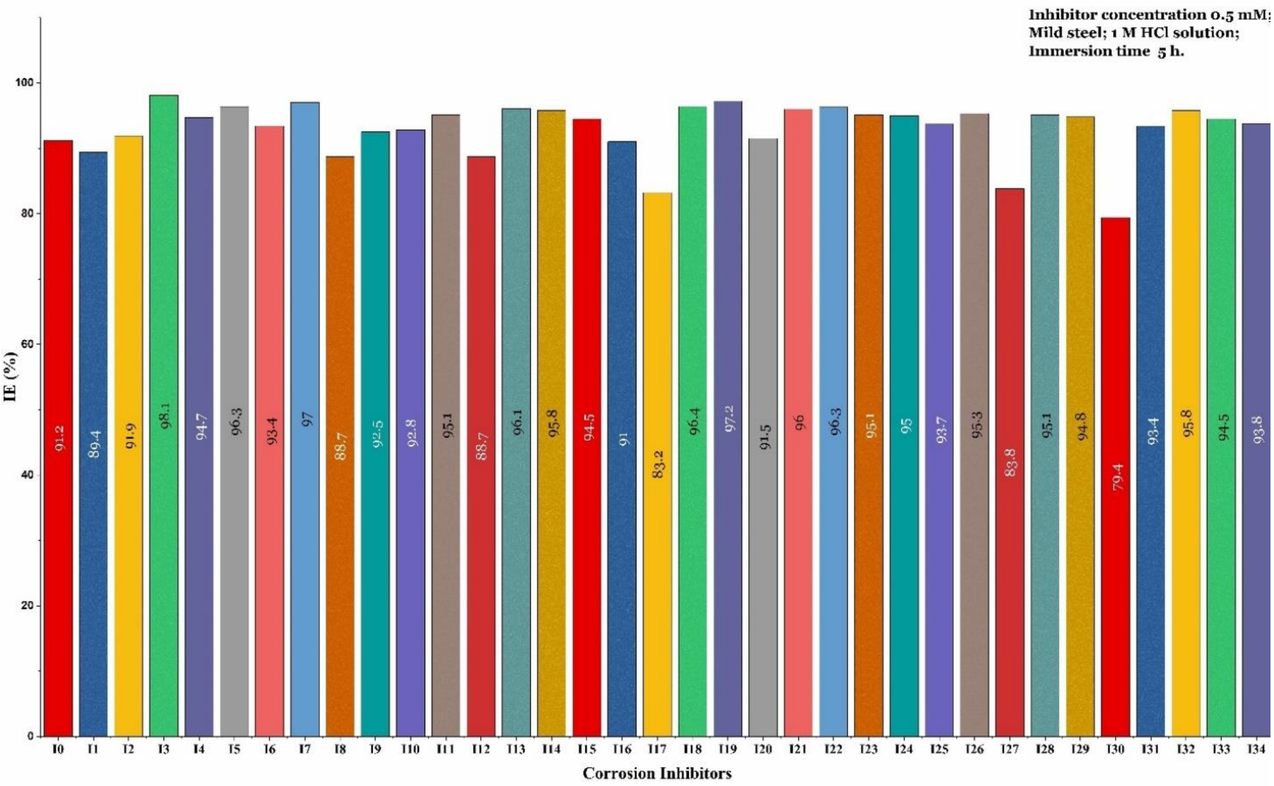

I0=PVA; I1= PVP; I2= N'-(2-(2-oxomethylpyrrol-1-yl)ethyl)piperidine [24]; I3= 2-Amino-4-phenyl-N-benzylidene-5-(1,2,4-triazol-1-yl)thiazole [25]; I4= 2-amino-4-phenylthiazole [26]; I5= 1-Amino-2-mercapto-5-(4-(pyrrol-1-yl)phenyl)-1,3,4-triazole [27]; I6= N'-(2-hydroxybenzylidene)-2-(quinolin-8-yloxy)acetohydrazide [28]; I7= 3-(4-ethyl-5-mercapto-1,2,4-triazol-3-yl)-1- phenylpropanone [29]; I8= 4-ethyl-1-(4-oxo-4-phenylbutanoyl)thiosemicarbazide [30];I9= 4-benzyl-1-(4-oxo-4-phenylbutanoyl)thiosemicarbazide [31]; I10=4-chloro-2-((pyridin-2-ylimino)methyl)phenol [32]; I11= 2-N-phenylamino-5-(3-phenyl-3-oxo-1-propyl)-1,3,4-oxadiazole [33]; I12= 4-ethyl-1-(4-oxo-4-phenylbutanoyl)thiosemicarbazide [34]; I13= 4-ethyl-1-(4-oxo-4-phenylbutanoyl)thiosemicarbazide [34]; I14= 4-pyrrol-1-yl-n-(2,5-dimethyl-pyrrol-1-yl)benzoylamine [35]; I15= N′-(1-phenylethyli-dene)-4-(1H-pyrrol-1-yl)benzohydrazide [35]; I16= 5-((4-fluorobenzylidene)amino)-1,3,4- thiadiazole-2-thiol [36]; I17= 2-(5-amino-1,3,4-thiadiazol-2-yl)-5-nitrofuran [37]; I18= terephthalo- hydrazide [38]; I19= isophthalohydrazide [33]; I20= N-(Naphthalen-1yl)-1-(4-pyridinyl)methanimine [39]; I21= 2-acetylthiophene thiosemicarbazon [40]; I22= 2-isonicotinoyl-N-phenylhydrazinecarbothioamide [41];I23= 2-amino-5-(naphthalen-2-ylmethyl)-1,3,4-thiadiazole[42]; I24= 5-(4-(1H-pyrrol-yl)phenyl)-2-mercapto-1,3,4-oxadiazole [43]; I25= N-(2,4-dihydroxytolueneylidene)-4-methylpyridin-2-amine [44]; I26= N-methyl-2-1-5-methylthiophene-2-yl)ethylidene) hydrazine carbothioamide [45]; I27= 1-phenyl-2-(1-phenylethylidene)hydrazine [46]; I28= 1-(1-(4-methoxyphenyl)ethylidene)-2-phenylhydrazine [46]; I29= 2-(2,4-dimethoxybenzylidene)-Nphenylhydrazin-e-carbothioamide [47]; I30= 2-(5-amino-1,3,4-oxadiazol-2-yl)-5-nitrofuran [48]; I31= 8-piperazine-1-ylmethylumbelliferone [49]; I32= 2-((6-methyl-2-ketoquinoUne-3-yl)methylene) hydrazinecarbothioamide [50]; I33= 4-(6-ethylcoumarin)acetohydrazide [51];I34= 4-(Benzoimidazole-2-yl)pyridine [52]; I35= 5,5′-(1,4-phenylene)bis(N-phenyl-1,3,4-thiadiazol-2-amine) [53].

Figure 8. The comparison of PVA and PVP with other published synthesized inhibitors as corrosion inhibitors.

3.2. Adsorption isotherm

The mechanism of interaction between PVA and PVP as corrosion inhibitors and metal surfaces can be easily understood through the use of adsorption isotherms. Gravimetric testing was used to determine the surface coverage (θ) values for PVA and PVP, which were then used to evaluate the most suitable isotherm model. The Temkin, Freundlich, and Langmuir isotherms were used to investigate the adsorption process. The particles of PVA and PVP may have adhered to the metal surfaces through physical or chemical adsorption. The results, as shown in Table 1, suggest that the Langmuir adsorption isotherm model was the best fit for both PVA and PVP, with regression coefficient (R^2) values of 0.99498 and 0.9923 respectively at 303 K. The estimated slope and intercept values for PVA and PVP are listed in Table 1, and the Langmuir isotherm plots between C_{inh}/θ and C_{inh} can be seen in Figures 9 and 10. The adsorption parameters can be calculated using Equation 4.

$$C_{\text{inh}} / \theta = (K_{\text{ads}})^{-1} + C \tag{4}$$

where C_{inh} is the concentration of PVA and PVP, θ is the surface area, and K_{ads} is the equilibrium constant.

The adsorption free energy ΔG^0_{ads} and K_{ads} were evaluated based on the plot between C/θ and C.

Equation 5 was used to calculate the adsorption parameters ΔG^0_{ads} and K_{ads}

$$\Delta G^0_{\text{ads}} = -RT \ln(55.5 K_{\text{ads}}) \tag{5}$$

where 55.5 is the molar concentration of water, R is the universal gas constant and T is absolute temperature.

The mechanism of chemisorption is determined by the value of ΔG^0_{ads}, which is -40 kJ·mol^{-1}, and more negative. On the other hand, a ΔG^0_{ads} value around -20 kJ·mol^{-1} and less negative is referred to as the mechanism of physisorption [54, 55]. The value of ΔG^0_{ads} for PVA is -29.85 kJ·mol^{-1} and for and PVP is -36.31 kJ·mol^{-1}, indicating the presence of both chemisorption and physisorption mechanisms.

Table 1. The thermodynamic parameters for PVA and PVP.

Inhibitor	**Parameter**	**303 K**	**313 K**	**323 K**	**333 K**
PVA	Intercept	0.101±0.016	0.118±0.015	0.135±0.017	0.165±0.029
	Slope	0.933±0.033	0.932±0.031	0.922±0.033	0.902±0.058
	R^2	0.994	0.995	0.994	0.983
PVP	Intercept	0.129±0.021	0.108±0.019	0.084±0.017	0.078±0.016
	Slope	0.949±0.041	0.970±0.0378	0.977±0.034	0.975±0.031
	R^2	0.99	0.993	0.995	0.995

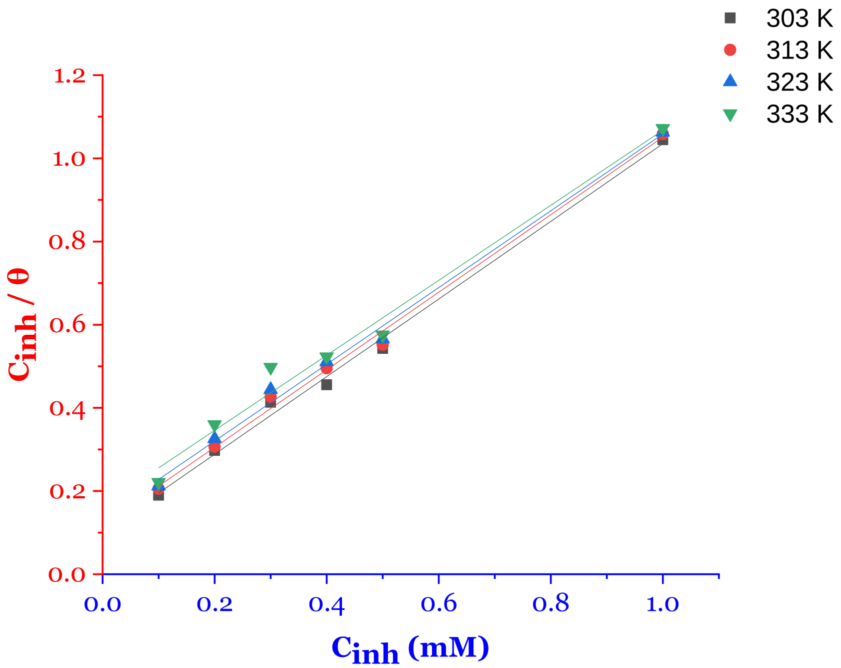

Figure 9. Langmuir isotherm of PVA plot for metallic coupon in inhibited acidic solution.

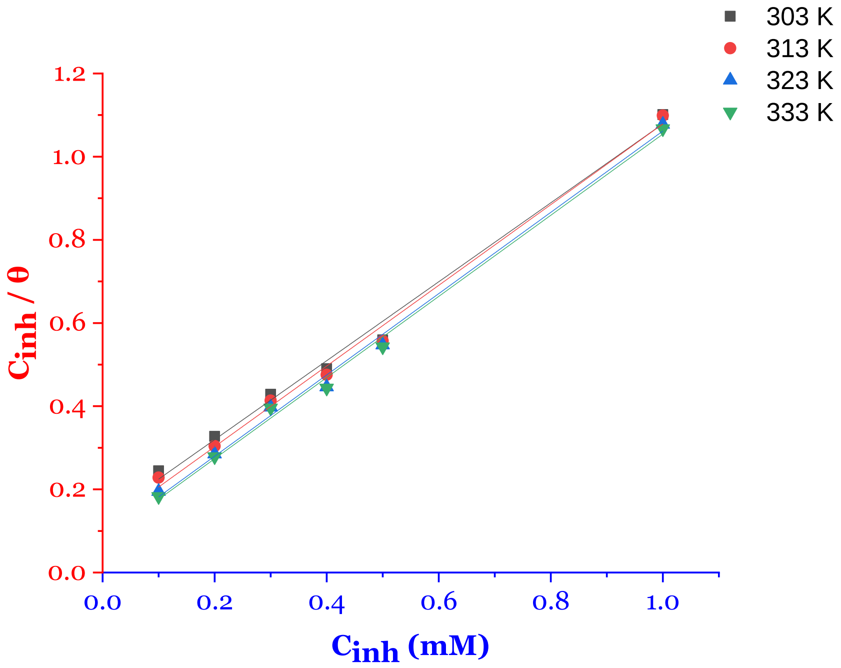

Figure 10. Langmuir isotherm of PVP plot for metallic coupon in inhibited acidic solution.

3.3. Surface analysis

Figure 11 demonstrates examples of SEM images of immersing steel material strips in untreated hydrochloric acid conditions. As depicted in Figure 11(a), the coupon surface endured substantial damage in the uninhibited solution, with numerous pits and fissures evident. However, when compared to the untreated solution, the metallic substrate surface in the solution treated with PVA and PVP showed remarkable improvement, with fewer cracks and pits as evident in Figure 11(b) and (c). The improvement is attributed to the protective coating formed on the metallic substrate surface, which blocks active sites and reduces the corrosion rate due to the presence of unpaired electron pair-containing oxygen (and nitrogen in the case of PVP) atoms.

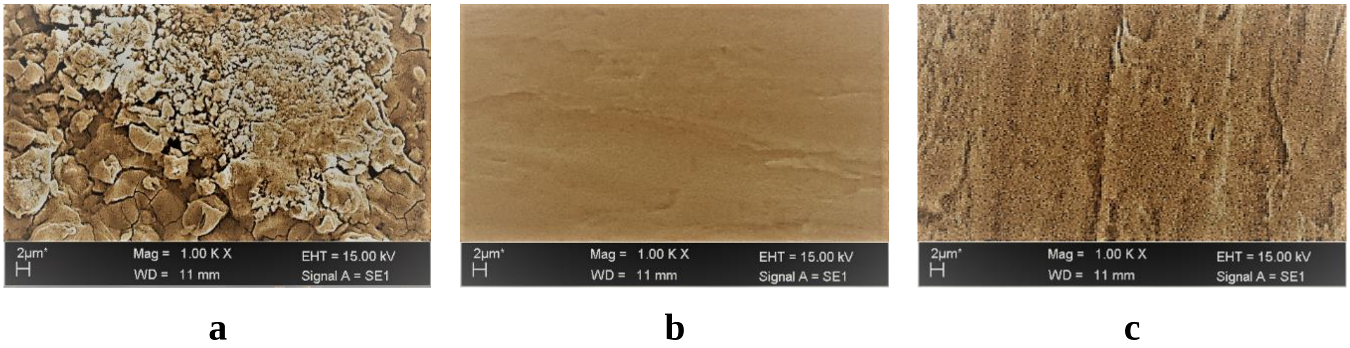

Figure 11. (a) demonstrates the SEM photograph of metallic substrate in treated medium, (b) demonstrates the SEM photograph of metallic substrate in treated medium with PVA, and (c) shows the SEM photograph of metallic substrate in treated medium with PVP.

3.4. Suggested inhibition mechanism by PVA and PVP

Organic inhibitors function by adsorbing onto the metal surface, effectively substituting themselves for other corrosive species and water molecules [56]. This process is influenced by various factors such as the state of the organic molecule in a corrosive environment and the charge on the metal surface [58]. Studies have shown that the steel surface in HCl solution carries a positive charge and absorbs chloride ions, which leads to the adsorption of cationic species [20, 56, 57].

PVA and PVP, when protonated in 1 M HCl solution, can be electrostatically adsorbed onto the metal surface through physisorption. Oxygen heteroatoms can be released from PVA and oxygen and nitrogen heteroatoms can be released from PVP on the surface, forming coordination and back-donating bonds through donor-acceptor interactions (chemisorption) [57]. Figures 12 and 13 depict the proposed inhibitory mechanisms for PVA and PVP, respectively, as potential inhibitors of mild steel corrosion in 1 M HCl solutions. The presence of PVA or PVP coatings on the mild steel surface prevents the penetration of corrosive ions, protecting the surface. The protective coating is believed to be created through the interaction of heteroatoms with the metal surface. The physical adsorption of the inhibitor molecules onto the mild steel surface is facilitated by the electrostatic interaction between the protonated PVA or PVP molecules and preabsorbed counter Cl^- ions, and the interaction between the inhibitor molecules′electron pairs and the iron's empty d-orbital [58].

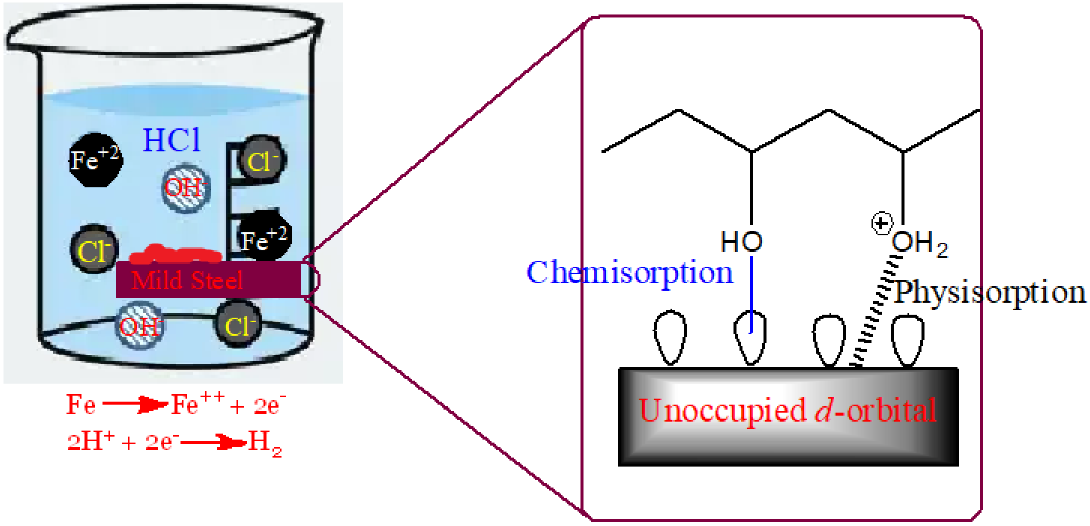

Figure 12. The suggested inhibitive mechanism of PVA.

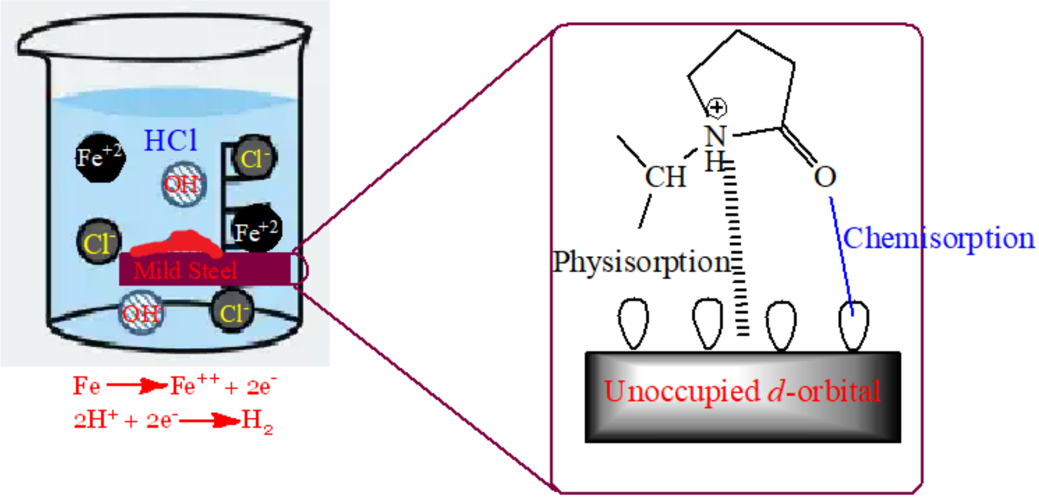

Figure 13. The suggested inhibitive mechanism of PVP.

Conclusion

An efficient and cost-effective strategy for mitigating corrosion is the use of corrosion inhibition technology. The increasing number of environmental lawsuits has spurred the development of environmentally friendly corrosion inhibitors. Mild steel corrosion inhibitors PVA and PVP have been investigated at temperatures ranging from 303 to 333 K in a 1 M HCl solution. The impact of varying concentrations and immersion times were also studied. The results showed that both PVA and PVP exhibit inhibitory effects on mild steel in the corrosive media, but PVA was found to be a superior inhibitor at 303 K while PVP performed better with rising temperatures. The weight-loss method showed that 0.5 mM PVA at 303 K protected the metal surface by 92.1%, while 0.5 mM PVP at the same temperature prevented corrosion by 89.4%. PVP's inhibition efficiency increased with an increase in temperature from 303 to 333 K, whereas PVA's inhibition efficiency decreased.

At 303 K, PVA's inhibitory efficacy started to decline, dropping from 92.1% at 303 K to 86.9% at 333 K, while PVP's inhibitory efficacy rose from 89.4% at 303 K to 92.1% at 333 K. SEM results confirmed that PVA and PVP are highly effective in delaying mild steel corrosion in 1 M HCl solution, which is in line with other research findings. The interaction between PVA and PVP with the steel substrate is explained by physisorption and chemical adsorption mechanisms, supporting the formation of complexes. PVA and PVP show great potential as ingredients in an acidic corrosion inhibitor.

References

1. N.K. Gupta, M.A. Quraishi, C. Verma and A.K. Mukherjee, Green Schiff's bases as corrosion inhibitors for mild steel in 1 M HCl solution: experimental and theoretical approach, *RSC Adv*., 2016, **6**, no. 104, 102076–102087. doi: 10.1039/C6RA22116E
2. K. Wan, P. Feng, B. Hou and Y. Li, Enhanced corrosion inhibition properties of carboxymethyl hydroxypropyl chitosan for mild steel in 1.0 M HCl solution, *RSC Adv*., 2016, **6**, no. 81, 77515–77524. doi: 10.1039/C6RA12975G
3. M. Bobina, A. Kellenberger, J.-P. Millet, C. Muntean and N. Vaszilcsin, Corrosion resistance of carbon steel in weak acid solutions in the presence of l-histidine as corrosion inhibitor, *Corros. Sci*., 2013, **69**, 389–395. doi: 10.1016/j.corsci.2012.12.020
4. K.R. Ansari and M.A. Quraishi, Experimental and quantum chemical evaluation of Schiff bases of isatin as a new and green corrosion inhibitors for mild steel in 20% H_2SO_4, *J. Taiwan Inst. Chem. Eng*., 2015, **54**, 145–154. doi: 10.1016/j.jtice.2015.03.013
5. A.A. Farag and M.A. Hegazy, Synergistic inhibition effect of potassium iodide and novel Schiff bases on X65 steel corrosion in 0.5 M H_2SO_4, *Corros. Sci*., 2013, **74**, 168–177. doi: 10.1016/j.corsci.2013.04.039
6. Sudheer and M.A. Quraishi, 2-Amino-3,5-dicarbonitrile-6-thio-pyridines: New and Effective Corrosion Inhibitors for Mild Steel in 1 M HCl, *Ind. Eng. Chem. Res*., 2014, **53**, 2851–2859. doi: 10.1021/ie401633y
7. B. Xu, Y. Ji, X. Zhang, X. Jin, W. Yang and Y. Chen, Experimental and theoretical studies on the corrosion inhibition performance of 4-amino-N,N-di-(2-pyridylmethyl)-aniline on mild steel in hydrochloric acid, *RSC Adv*., 2015, **5**, no. 69, 56049–56059. doi: 10.1039/C5RA09173J
8. Y. Ji, B. Xu, W. Gong, X. Zhang, X. Jin, W. Ning, Y. Meng, W. Yang and Y. Chen, Corrosion inhibition of a new Schiff base derivative with two pyridine rings on Q235 mild steel in 1.0 M HCl, *J. Taiwan Inst. Chem. Eng*., 2016, **66**, 301–312. doi: 10.1016/j.jtice.2016.07.007
9. L.O. Olasunkanmi, I.B. Obot and E.E. Ebenso, Adsorption and corrosion inhibition properties of N-{n-[1-R-5-(quinoxalin-6-yl)-4,5-dihydropyrazol-3-yl]phenyl} methanesulfonamides on mild steel in 1 M HCl: experimental and theoretical studies, *RSC Adv*., 2016, **6**, no. 90, 86782–86797. doi: 10.1039/C6RA11373G

10. S. Junaedi, A.A.H. Kadhum, A. Al-Amiery, A.B. Mohamad and M.S. Takriff, Synthesis and Characterization of Novel Corrosion Inhibitor Derived from Oleic acid: 2-Amino-5-Oleyl 1,3,4-Thiadiazol (AOT), *Int. J. Electrochem. Sci*., 2012, **7**, 3543–3554.
11. H.S. Aljibori, A.H. Alwazir, S. Abdulhadi, W.K. Al-Azzawi, A.A.H. Kadhum, L.M. Shaker, A.A. Al-Amiery and H.Sh. Majdi, The use of a Schiff base derivative to inhibit mild steel corrosion in 1 M HCl solution: a comparison of practical and theoretical findings, *Int. J. Corros. Scale Inhib*., 2022, **11**, no. 4, 1435–1455. doi: 10.17675/2305-6894-2022-11-4-2
12. W.K. Al-Azzawi, S.M. Salih, A.F. Hamood, R.K. Al-Azzawi, M.H. Kzar, H.N. Jawoosh, L.M. Shakier, A. Al-Amiery, A.A.H. Kadhum, W.N.R.W. Isahak and M.S. Takriff, Adsorption and theoretical investigations of a Schiff base for corrosion inhibition of mild steel in an acidic environment, *Int. J. Corros. Scale Inhib*., 2022, **11**, no. 3, 1063–1082. doi: 10.17675/2305-6894-2022-11-3-10
13. D.M. Jamil, A.K. Al-Okbi, M.M. Hanon, K.S. Rida, A.F. Alkaim, A.A. Al-Amiery, A. Kadhum and A.A.H. Kadhum, Carbethoxythiazole corrosion inhibitor: as an experimentally model and DFT theory, *J. Eng. Appl. Sci*., 2018, **13**, no. 11, 3952–3959. doi: 10.36478/jeasci.2018.3952.3959
14. A.H. Alobaidy, A. Kadhum, S.B. Al-Baghdadi, A.A. Al-Amiery, A.A.H. Kadhum, E. Yousif and A.B. Mohamad, Eco-friendly corrosion inhibitor: experimental studies on the corrosion inhibition performance of creatinine for mild steel in HCl complemented with quantum chemical calculations, *Int. J. Electrochem. Sci*., 2015, **10**, 3961–3972.
15. S. Subhashini and A.F. Sabirneeza, Gravimetric and electrochemical investigation of water soluble poly(vinyl alcohol-threonine) as corrosion inhibitor for mild steel, *In: Proceedings of WCECS*, 2011, **2**, 657–662.
16. S.A. Umoren, M.M. Solomon, S.A. Ali and H.D.M. Dafalla, Synthesis, characterization, and utilization of a diallylmethylamine-based cyclopolymer for corrosion mitigation in simulated acidizing environment, *Mater. Sci. Eng.: C*, 2019, **100**, 897–914. doi: 10.1016/j.msec.2019.03.057
17. ASTM, G 31–72, American Society for Testing and Materials, Philadelphia, PA, 1990.
18. NACE Standard TM 0169/G31–12a. (2012). Standard Guide for Laboratory Immersion Corrosion Testing of Metals.
19. S.B. Al-Bghdadi, M.M. Hanoon, J.F. Odah, L.M. Shaker and A.A. Al-Amiery, Benzylidene as Efficient Corrosion Inhibition of Mild Steel in Acidic Solution. Proceedings, 2019, **41**, no. 1, 27. doi: 10.3390/ecsoc-23-06472
20. M.M. Solomon, S.A. Umoren, M.A. Quraishi, D. Tripathi and E.J. Abai, Effect of akyl chain length, flow, and temperature on the corrosion inhibition of carbon steel in a simulated acidizing environment by an imidazoline-based inhibitor, *J. Pet. Sci. Eng*., 2020, **187**, 106801. doi: 10.1016/j.petrol.2019.106801

21. B.S. Mahdi, H.S.S. Aljibori, M.K. Abbass, W.K. Al-Azzawi, A.H. Kadhum, M.M. Hanoon, W.N.R.W. Isahak, A.A. Al-Amiery and H.Sh. Majdi, Gravimetric analysis and quantum chemical assessment of 4-aminoantipyrine derivatives as corrosion inhibitors, *Int. J. Corros. Scale Inhib.*, 2022, **11**, no. 3, 1191–1213. doi: 10.17675/2305-6894-2022-11-3-17
22. A.A. Alamiery, Study of Corrosion Behavior of N′-(2-(2-oxomethylpyrrol-1-yl) ethyl)piperidine for Mild Steel in the Acid Environment, *Biointerface Res. Appl. Chem.*, 2022, **12**, no. 3, 3638–3646. doi: 10.33263/BRIAC123.36383646
23. A. Alamiery, A.B. Mohamad, A.A.H. Kadhum and M.S. Takriff, Comparative data on corrosion protection of mild steel in HCl using two new thiazoles, *Data Brief*, 2022, **40**, 107838. doi: 10.1016/j.dib.2022.107838
24. A.M. Mustafa, F.F. Sayyid, N. Betti, L.M. Shaker, M.M. Hanoon, A.A. Alamiery, A.A.H. Kadhum and M.S. Takriff, Inhibition of mild steel corrosion in hydrochloric acid environment by 1-amino-2-mercapto-5-(4-(pyrrol-1-yl)phenyl)-1,3,4-triazole, *S. Afr. J. Chem. Eng.*, 2022, **39**, 42–51. doi: 10.1016/j.sajce.2021.11.009
25. A.A. Alamiery, Investigations on corrosion inhibitory effect of newly quinoline derivative on mild steel in HCl solution complemented with antibacterial studies, *Biointerface Res. Appl. Chem.*, 2022, **12**, no. 2, 1561–1568. doi: 10.33263/BRIAC122.15611568
26. I.A. Alkadir Aziz, I.A. Annon, M.H. Abdulkareem, M.M. Hanoon, M.H. Alkaabi, L.M. Shaker, A.A. Alamiery, W.N.R.W. Isahak and M.S. Takriff, Insights into Corrosion Inhibition Behavior of a 5-Mercapto-1,2,4-triazole Derivative for Mild Steel in Hydrochloric Acid Solution: Experimental and DFT Studies, *Lubricants*, 2021, **9**, no. 12, 122. doi: 10.3390/lubricants9120122
27. A.A. Alamiery, Short report of mild steel corrosion in 0.5 M H_2SO_4 by 4-ethyl-1-(4-oxo4-phenylbutanoyl)thiosemicarbazide, *Jurnal Tribologi*, 2021, **30**, 90–99.
28. A.A. Alamiery, W.N.R.W. Isahak and M.S. Takriff, Inhibition of mild steel corrosion by 4-benzyl-1-(4-oxo-4-phenylbutanoyl)thiosemicarbazide: Gravimetrical, adsorption and theoretical studies, *Lubricants*, 2021, **9**, no. 9, 93. doi: 10.3390/lubricants9090093
29. M.A. Dawood, Z.M.K. Alasady, M.S. Abdulazeez, D.S. Ahmed, G.M. Sulaiman, A.A.H. Kadhum, L.M. Shaker and A.A. Alamiery, The corrosion inhibition effect of a pyridine derivative for low carbon steel in 1 M HCl medium: Complemented with antibacterial studies, *Int. J. Corros. Scale Inhib.*, 2021, **10**, no. 4, 1766–1782. doi: 10.17675/2305-6894-2021-10-4-25
30. A.A. Alamiery, Corrosion inhibition effect of 2-N-phenylamino-5-(3-phenyl-3-oxo-1-propyl)-1,3,4-oxadiazole on mild steel in 1 M hydrochloric acid medium: Insight from gravimetric and DFT investigations, *Mater. Sci. Energy Technol.*, 2021, **4**, 398–406. doi: 10.1016/j.mset.2021.09.002
31. A.A. Alamiery, Anticorrosion effect of thiosemicarbazide derivative on mild steel in 1 M hydrochloric acid and 0.5 M sulfuric Acid: Gravimetrical and theoretical studies, *Mater. Sci. Energy Technol.*, 2021, **4**, 263–273. doi: 10.1016/j.mset.2021.07.004

32. A.A. Alamiery, W.N.R.W. Isahak, H.S.S. Aljibori, H.A. Al-Asadi and A.A.H. Kadhum, Effect of the structure, immersion time and temperature on the corrosion inhibition of 4-pyrrol-1-yl-N-(2,5-dimethyl-pyrrol-1-yl)benzoylamine in 1.0 M HCl solution, *Int. J. Corros. Scale Inhib.*, 2021, **10**, 700–713. doi: 10.17675/2305-6894-2021-10-2-14
33. A.A. Alamiery, E. Mahmoudi and T. Allami, Corrosion inhibition of low-carbon steel in hydrochloric acid environment using a Schiff base derived from pyrrole: gravimetric and computational studies, *Int. J. Corros. Scale Inhib.*, 2021, **10**, no. 2, 749–765. doi: 10.17675/2305-6894-2021-10-2-17
34. A.J.M. Eltmimi, A. Alamiery, A.J. Allami, R.M. Yusop, A.H. Kadhum and T. Allami, Inhibitive effects of a novel efficient Schiff base on mild steel in hydrochloric acid environment, *Int. J. Corros. Scale Inhib.*, 2021, **10**, no. 2, 634–648. doi: 10.17675/2305-6894- 2021-10-2-10
35. A. Alamiery, L.M. Shaker, T. Allami, A.H. Kadhum and M.S. Takriff, A study of acidic corrosion behavior of Furan-Derived schiff base for mild steel in hydrochloric acid environment: Experimental, and surface investigation, *Mater. Today: Proc.*, 2021, **44**, 2337–2341. doi: 10.1016/j.matpr.2020.12.431
36. S. Al-Baghdadi, A. Al-Amiery, T. Gaaz and A. Kadhum, Terephthalohydrazide and isophthalo-hydrazide as new corrosion inhibitors for mild steel in hydrochloric acid: Experimental and theoretical approaches, *Koroze Ochr. Mater.*, 2021, **65**, 12–22. doi: 10.2478/kom-2021-0002
37. M.M. Hanoon, A.M. Resen, L.M. Shaker, A.A.H. Kadhum and A.A. Al-Amiery, Corrosion investigation of mild steel in aqueous hydrochloric acid environment using N-(naphthalen-1yl)-1-(4-pyridinyl)methanimine complemented with antibacterial studies, *Biointerface Res. Appl. Chem.*, 2021, **11**, no. 2, 9735–9743. doi: 10.33263/BRIAC112.97359743
38. S. Al-Baghdadi, T.S. Gaaz, A. Al-Adili, A.A. Al-Amiery and M.S. Takriff, Experimental studies on corrosion inhibition performance of acetylthiophene thiosemicarbazone for mild steel in HCl complemented with DFT investigation, *Int. J. Low-Carbon Technol.*, 2021, **16**, no. 1, 181–188. doi: 10.1093/ijlct/ctaa050
39. A.A. Al-Amiery, Anti-corrosion performance of 2-isonicotinoyl-N-phenylhydrazinecarbothioamide for mild steel hydrochloric acid solution: Insights from experimental measurements and quantum chemical calculations, *Surf. Rev. Lett.*, 2021, **28**, no. 3, 2050058. doi.: 10.1142/S0218625X20500584
40. M.S. Abdulazeez, Z.S. Abdullahe, M.A. Dawood, Z.K. Handel, R.I. Mahmood, S. Osamah, A.H. Kadhum, L.M. Shaker and A.A. Al-Amiery, Corrosion inhibition of low carbon steel in HCl medium using a thiadiazole derivative: weight loss, DFT studies and antibacterial studies, *Int. J. Corros. Scale Inhib.*, 2021, **10**, no. 4, 1812–1828. doi: 10.17675/2305-6894-2021-10-4-27

41. A.M. Mustafa, F.F. Sayyid, N. Betti, M.M. Hanoon, A. Al-Amiery, A.A.H. Kadhum and M.S. Takriff, Inhibition Evaluation of 5-(4-(1H-pyrrol-1-yl)phenyl)-2-mercapto-1,3,4-oxadiazole for the Corrosion of Mild Steel in an Acid environment: Thermodynamic and DFT Aspects, *Tribologia*, 2021, **38**, no. 3–4, 39–47. doi: 10.30678/fjt.105330
42. Y.M. Abdulsahib, A.J.M. Eltmimi, S.A. Alhabeeb, M.M. Hanoon, A.A. Al-Amiery, T. Allami and A.A.H. Kadhum, Experimental and theoretical investigations on the inhibition efficiency of N-(2,4-dihydroxytolueneylidene)-4-methylpyridin-2-amine for the corrosion of mild steel in hydrochloric acid, *Int. J. Corros. Scale Inhib.*, 2021, **10**, no. 3, 885–899. doi: 10.17675/2305-6894-2021-10-3-3
43. A.K. Khudhair, A.M. Mustafa, M.M. Hanoon, A. Al-Amiery, L.M. Shaker, T. Gazz, A.B. Mohamad, A.H. Kadhum and M.S. Takriff, Experimental and Theoretical Investigation on the Corrosion Inhibitor Potential of N-MEH for Mild Steel in HCl, *Prog. Color Colorants Coat.*, 2022, **15**, no. 2, 111–122. doi: 10.30509/pccc.2021.166815.1111
44. D.S. Zinad, R.D. Salim, N. Betti, L.M. Shaker and A.A. AL-Amiery, Comparative Investigations of the Corrosion Inhibition Efficiency of a 1-phenyl-2-(1-phenylethylidene)hydrazine and its Analog Against Mild Steel Corrosion in Hydrochloric Acid Solution, *Prog. Color, Colorants Coat.*, 2022, **15**, no. 1, 53–63. doi: 10.30509/pccc.2021.166786.1108
45. R.D. Salim, N. Betti, M. Hanoon and A.A. Al-Amiery, 2-(2,4-Dimethoxybenzylidene)-N-Phenylhydrazinecarbothioamide as an Efficient Corrosion Inhibitor for Mild Steel in Acidic Environment, *Prog. Color, Colorants Coat.*, 2022, **15**, no. 1, 45–52. doi: 10.30509/pccc.2021.166775.1105
46. A.A. Al-Amiery, L.M. Shaker, A.H. Kadhum and M.S. Takriff, Exploration of furan derivative for application as corrosion inhibitor for mild steel in hydrochloric acid solution: Effect of immersion time and temperature on efficiency, *Mater. Today: Proc.*, 2021, **42**, 2968–2973. doi: 10.1016/j.matpr.2020.12.807
47. A.M. Resen, M.M. Hanoon, W.K. Alani, A. Kadhim, A.A. Mohammed, T.S. Gaaz, A.A.H. Kadhum, A.A. Al-Amiery and M.S. Takriff, Exploration of 8-piperazine-1-ylmethylumbelliferone for application as a corrosion inhibitor for mild steel in hydrochloric acid solution, *Int. J. Corros. Scale Inhib.*, 2021, **10**, no. 1, 368–387. doi: 10.17675/2305-6894-2021-10-1-21
48. M.M. Hanoon, A.M. Resen, A.A. Al-Amiery, A.A.H. Kadhum and M.S. Takriff, Theoretical and Experimental Studies on the Corrosion Inhibition Potentials of 2-((6-Methyl-2-Ketoquinolin-3-yl)Methylene) Hydrazinecarbothioamide for Mild Steel in 1 M HCl, *Prog. Color, Colorants Coat.*, 2021, **15**, no. 1, 11–23. doi: 10.30509/pccc.2020.166739.1095
49. F.G. Hashim, T.A. Salman, S.B. Al-Baghdadi, T. Gaaz and A. Al-Amiery, Inhibition effect of hydrazine-derived coumarin on a mild steel surface in hydrochloric acid, *Tribologia*, 2020, **37**, no. 3–4, 45–53. doi: 10.30678/fjt.95510

50. A.M. Resen, M.M. Hanoon, R.D. Salim, A.A. Al-Amiery, L.M. Shaker and A.A.H. Kadhum, Gravimetrical, theoretical, and surface morphological investigations of corrosion inhibition effect of 4-(benzoimidazole-2-yl) pyridine on mild steel in hydrochloric acid, *Koroze Ochr. Mater*., 2020, **64**, 122–130. doi: 10.2478/kom-2020-0018
51. A.Z. Salman, Q.A. Jawad, K.S. Ridah, L.M. Shaker and A.A. Al-Amiery, Selected BIS-Thiadiazole: Synthesis and Corrosion Inhibition Studies on Mild Steel in HCL Environment, *Surf. Rev. Lett*., 2020, **27**, no. 12, 2050014. doi: 10.1142/S0218625X20500146
52. S. Junaedi, A.A. Al-Amiery, A. Kadhum, A.A.H. Kadhum and A.B. Mohamad, Inhibition effects of a synthesized novel 4-aminoantipyrine derivative on the corrosion of mild steel in hydrochloric acid solution together with quantum chemical studies, *Int. J. Mol. Sci*., 2013, **14**, no. 6, 11915–11928. doi: 10.3390/ijms140611915
53. A.A. Alamiery, W.N.R.W. Isahak, H.S.S. Aljibori, H.A. Al-Asadi and A.A.H. Kadhum, Effect of the structure, immersion time and temperature on the corrosion inhibition of 4-pyrrol-1-yl-N-(2,5-dimethyl-pyrrol-1-yl)benzoylamine in 1.0 M HCL solution, *Int. J. Corros. Scale Inhib*., 2021, **10**, no. 2, 700–713. doi: 10.17675/2305-6894-2021-10-2-14
54. S. Al-Baghdadi, F.G. Hashim, A.Q. Salam, T.K. Abed, T.S. Gaaz, A.A. Al-Amiery, A.A.H. Kadhum, K.S. Reda and W.K. Ahmed, Synthesis and corrosion inhibition application of NATN on mild steel surface in acidic media complemented with DFT studies, *Results Phys*., 2018, **8**, 1178–1184. doi: 10.1016/j.rinp.2018.02.007
55. H.M. Abd El-Lateef, Corrosion inhibition characteristics of a novel salycilidene isatin hydrazine sodium sulfonate on carbon steel in hcl and a synergistic nickel ions additive: A combined experimental and theoretical perspective, *Appl. Surf. Sci*., 2020, **501**, 144237. doi: 10.1016/j.apsusc.2019.144237
56. I.B. Onyeachu, I.B. Obot, A.A. Sorour and M.I. Abdul-Rashid, Green corrosion inhibitor for oilfield application I: electrochemical assessment of 2-(2-pyridyl) benzimidazole for API X60 steel under sweet environment in NACE brine ID196, *Corros. Sci*., 2019, **150**, 183–193. doi: 10.1016/j.corsci.2019.02.010
57. S.A. Umoren and M.M. Solomon, Protective polymeric films for industrial substrates: A critical review on past and recent applications with conducting polymers and polymer composites/nanocomposites, *Prog. Mater. Sci*., 2019, **104**, 380–450. doi: 10.1016/j.pmatsci.2019.04.002
58. W.K. Al-Azzawi, A.J. Al Adily, F.F. Sayyid, R.K. Al-Azzawi, M.H. Kzar, H.N. Jawoosh, A.A. Al-Amiery, A.A.H. Kadhum, W.N.R.W. Isahak and M.S. Takriff, Evaluation of corrosion inhibition characteristics of an N-propionanilide derivative for mild steel in 1 M HCl: Gravimetrical and computational studies, *Int. J. Corros. Scale Inhib*., 2022, **11**, no. 3, 1100–1114. doi: 10.17675/2305-6894-2022-11-3-12

◆ ◆ ◆